Defence Science Journal, Vol 46, No 5, November 1996, pp. 347-360

A Review of the Thermal Decomposition Pathways in RDX, HMX and Other Closely Related Cyclic Nitramines.

Suryanarayana Bulusu
US Army Armaments Research, Development and Engineering Center
Picatinny Arsenal, NJ 07806

and

Richard Behrens, Jr.
Combustion Research Facility, Sandia National Laboratories
Livermore, CA 94551

ABSTRACT

Understanding the complex physicochemical processes involved in the combustion and decomposition of energetic materials is essential to the development of reliable models for the performance, stability and hazards analysis of propellants and explosives and to provide a basis for improvement of ignition and sensitivity properties of their formulations. Since the nitramines RDX and HMX are important materials as propellants and explosives, we have undertaken a comprehensive, in-depth study, over the years, of their thermal decomposition kinetics and mechanisms using unusual sophisticated techniques, namely, simultaneous thermogravimetric modulated beam mass spectrometry (STMBMS), time-of-flight velocity spectra analysis, isotope labeling (^{15}N, ^{13}C, ^{2}H and ^{18}O), isotope scrambling techniques and deuterium kinetic isotope effects (DKIE). In this paper, the results of the condensed and gas phase decomposition studies of RDX and HMX are reviewed in terms of the reaction pathways, bond-breaking steps and some bond-forming reactions. A comparison is made with the decomposition of six other cyclic nitramines and the common and contrasting modes of decomposition are highlighted. In particular, it is shown that the formation of a mononitroso analogue from RDX and HMX, respectively, as intermediates, represents an important thermal degradation pathway in each and probably also in four other nitramines studied. The cyclic nitramine 1,3,5-trinitro-1,3,5-triaza-cyclo-heptane exhibits the potential to be a new useful nitramine with valuable applications.

1. INTRODUCTION

The cyclic nitramines hexahydro-1,3,5-trinitro-s-triazine, RDX (I) and octahydro-1,3,5,7-tetranitro-1,3,5,7-tetraazocine, HMX (II) are high energy containing compounds that are used extensively in both propellant and explosive formulations. A thorough knowledge of the underlying complex physico-chemical processes in the combustion of these materials is essential to develop methods to modify their formulations so as to obtain better ignition, combustion or sensitivity properties. There are several other less known cyclic nitramines also described in the literature which are structurally similar to RDX and HMX, some of which are covered in this review; Their structures are shown in Fig. 1. A detailed study of the decomposition processes of these materials serves several purposes. Firstly, in solid-propellant combustion, the decomposition processes occurring in the condensed

Received 02 September 1996

phase generate low molecular weight chemical species that feed the gas phase flames. These processes together control the burn rates of propellants. Secondly, in both propellants and explosives it is important to understand the mechanisms that control the stability of these materials when they are subjected to elevated temperatures, electrostatic discharge, impact or shock. The response of energetic materials to these stimuli determines their degree of safety when subjected to abnormal environments such as fires. Thirdly, a knowledge of the molecular processes that control the response of the energetic materials to abnormal environments will provide an insight into the molecular properties which control the relative stability and sensitivity of these materials. Finally, a comparison of the decomposition pathways of a variety of cyclic nitramines should shed some light on the structural factors that promote stability and other desirable properties.

Until about ten years ago there were scattered reports on investigations of the decomposition chemistry of RDX and HMX which included slow-heating rate studies,[1-4] mass spectrometry studies,[5-9] high-heating rate studies[10,11] and studies of shock intiated decomposition[12,13]. These studies were recently reviewed[14,15] in the literature. The current work in these laboratories over the last ten years being reviewed now, has utilised more sophisticated experimental techniques namely, simultaneous thermogravimetric modulated beam mass spectrometry (STMBMS)[16], time-of-flight velocity spectra analysis, isotope labeling (^{15}N, ^{13}C, ^{2}H and ^{18}O), isotope scrambling techniques[17-20] and deuterium kinetic isotope effects (DKIE)[17-20] to investigate the kinetics of decomposition and the initial work focussed on RDX and HMX decompositions[17-20]. Following this work, less extensive investigations have been carried out on the nitramines (III) to (VIII) (Fig.1) in an effort to obtain structural correlations[21-23]. The highlights of these investigations on RDX, HMX and the other cyclic nitramines in Fig. 1, are presented in this paper with the focus on the common features as well as the significant differences.

2. EXPERIMENTAL METHODS & MATERIALS

2.1 Experimental Methods

Various experimental techniques employed in obtaining the quantitative and qualitative data on the nitramine decompositions are already described in great detail in References 16 to 23. Therefore, merely a brief outline of the methods will be included here. Thermal decomposition measurements in these studies are carried out on typically 2 to 10 mg samples using the STMBMS apparatus[16].

This apparatus basically consists of a thermo-balance, a specially designed alumina reaction cell in which the decomposition is carried out and a quadrupole mass spectrometer with the ionisation source vertically above the reaction cell. The molecules that exit the cell into a high vacuum environment (~10^{-6} to 10^{-10} torr), are formed into a modulated molecular beam and pass directly through the electron-bombardment ionizer of a quadrupole mass spectrometer without undergoing any further collisions with background

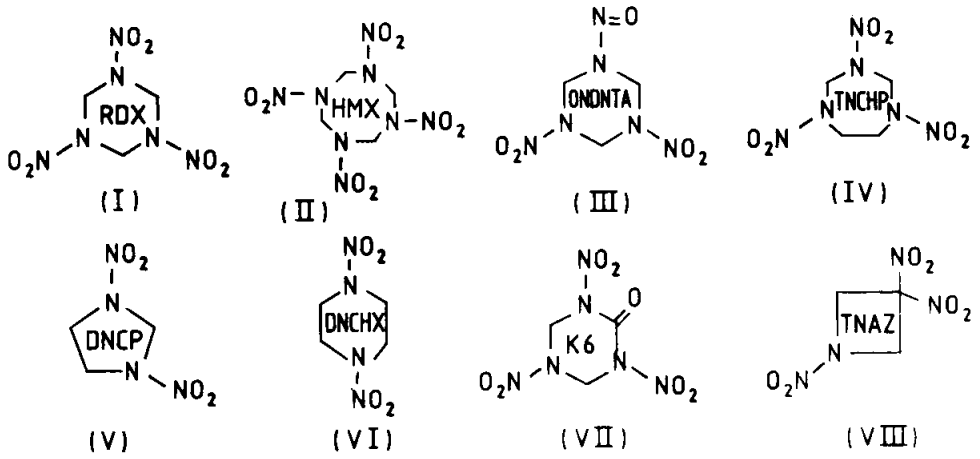

Figure 1. Structures of nitramines currently under investigation.

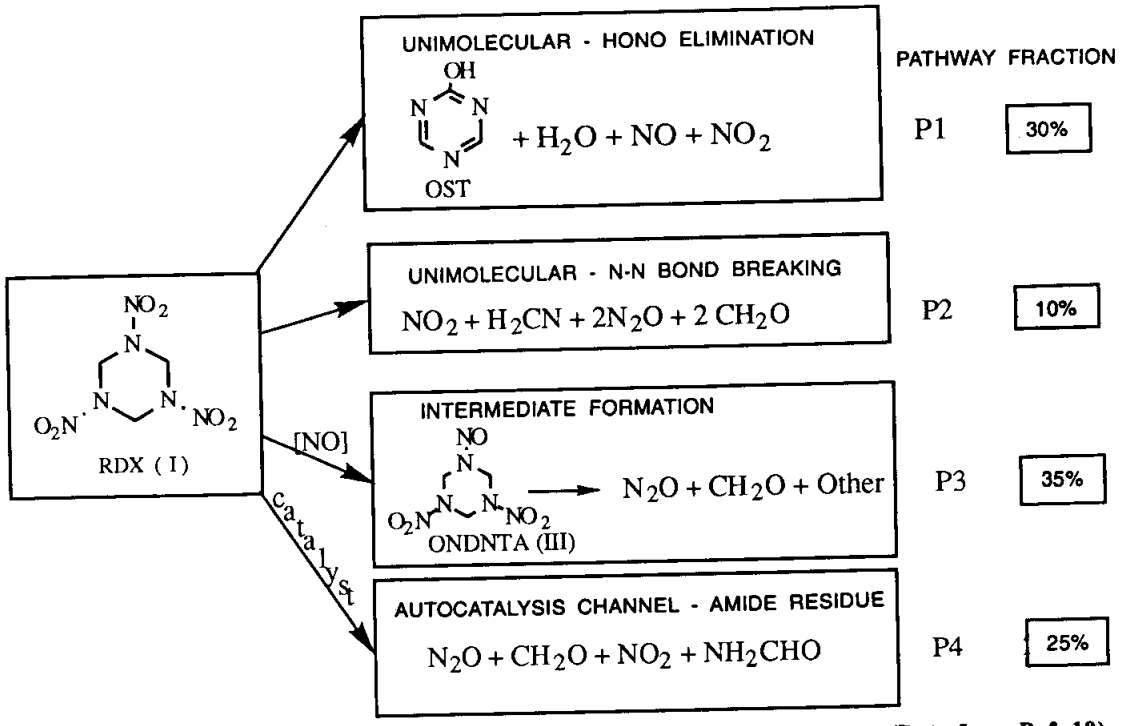

Figure 2. Four major decomposition pathways of RDX in the liquid Phase. (Data from Ref. 19) behavior of the products formed during the thermal decomposition of TNAZ-1-$^{15}NO_2$.

molecules or walls of the vacuum chamber. In the region between the reaction cell and the ionization source are located a set of beam defining orifices and a beam modulating wheel. This instrument allows the gas-phase species to be identified and their rates of formation to be measured as a function of time. The decomposition is carried out in the alumina reaction cell from which the gaseous decomposition products may exit only through an orifice whose diameter ranges from 2.5 μm to 1000 μm depending upon the degree of confinement of the decomposition products desired (pressure of the contained gases can be varied between 0 and 2000 torr). The force due to the gas within and exiting the reaction cell (thrust and mass loss) is measured simultaneously with the mass spectra of the evolving gases. The gases are identified from the m/z values of temporally correlated groups of ion signals, from the molecular weight of the neutral molecules evolving from the cell as determined from time-of-flight velocity spectra and by use of isotopically tagged analogues of the molecules being studied. The rates of gas formation are determined in an analysis procedure that utilises the ion signals measured with the mass spectrometer, the force measured by the microbalance and the flow characteristics of the reaction cell orifice. The end result of the experiments and the data analysis procedure is the rate of gas formation of each species formed during the thermal decomposition as a function of time and of pressure of the contained gases. From this information, insight into the reaction mechanisms that control the decomposition process and the kinetic rate parameters associated with the rate controlling reaction mechanisms is obtained.

2.2 Source of Samples Studied

While RDX and HMX samples were obtained from military sources and purified by repeatedcrystallisations from acetone, their isotopic analogues and all the other nitramines were made in these laboratories by methods already known. The syntheses of the isotopic analogues of RDX (I) and HMX (II) were described in previous papers[20,24]. ONDNTA (III) and its deuterium labeled analogue, ONDNTA-d_6, which are intermediates in the decomposition of RDX and RDX-d_6 respectively, were prepared according to previously known methods[25] starting with the corresponding hexahydro-1,3,5-trinitroso-s-triazine analogue. The deuterated version of the hexahydro-1,3,5-trinitroso-s-triazine was prepared by the base catalysed deuterium exchange method described in yet another paper[26]. The nitramines TNCHP[27] (IV), DNCP[28] (V) and DNCHX[29] (VI) were synthesised according to the methods already described

in the early literature on nitramines. The methods of synthesis of K6[30] (VII) and TNAZ [31] (VIII) were also published relatively recently. $^{15}NO_2$-labeled TNAZ was prepared by treating 3,3-dinitroazetidine, an intermediate in the TNAZ synthesis, with $H^{15}NO3$.

3. RDX & HMX DECOMPOSITIONS

The decomposition of both RDX and HMX is controlled by multiple pathways whose behaviour depends on the physical state of the sample. In the case of RDX, for example, four major pathways shown in Fig. 2 have been identified[19]. The decomposition of both RDX[19,20] and HMX[17,18] gives rise to many common products, the nature and relative abundance of each being determined by initial decomposition reactions (i.e., *N-NO2* bond breaking and *HONO* elimination) and secondary reactions between the reactant and its decomposition products. Examples of common products are H_2O, N_2O, CH_2O, *NO*, *CO*, *HCN*, NO_2, NH_2CHO and CH_3NHCHO. Products unique to each are OST (oxy-s-triazine, m/z 97), ONDNTA (m/z 206) from RDX and ONTNTA and $(CH_3)_2N$-*NO* from HMX : One important common pathway of decomposition in both RDX and HMX was found[17-19] to be the formation of the mononitroso analogues (1-nitroso-3,5-dinitro-1,3,5-triazine, ONDNTA (III) and 1-nitroso-3,5,7-trinitro-1,3,5,7-tetraazocine, ONTNTA, respectively) of these cyclic nitramines as intermediates in both liquid and solid phases. Isotope scrambling experiments using mixtures of fully ^{15}N-labeled and unlabeled samples showed that the mononitroso analogues were formed with complete isotope mixing in the liquid phase decompositions and partial mixing in the solid phase decompositions. This implies a re-formation of *N-NO* bond at least in the liquid phase decomposition pathways. Both ONDNTA and ONTNTA undergo further decomposition, contributing to the low molecular weight gaseous products observed in the RDX and HMX decompositions and, therefore, play a significant role in the overall decomposition processes.

3.1 RDX Decomposition in the Liquid Phase

Of the four primary reaction pathways controlling the decomposition of RDX in the liquid phase between 200 and 215 °C (Fig. 2), two pathways are "first order" reactions solely in RDX. One of these produces predominantly OST, *NO*, and H_2O and accounts for approximately 30 per cent of the decomposed RDX and the other produces predominantly N_2O and CH_2O with smaller amounts of NO_2, *CO*, and NH_2CHO and accounts for 10 per cent of the decomposed RDX. The third pathway consists of formation of ONDNTA by reaction between *NO* and RDX, followed by the decomposition of ONDNTA to predominantly CH_2O and N_2O. The nature of the fourth reaction pathway is less certain. From our original experiments on RDX, we proposed that in the fourth pathway, RDX decomposes by reaction with a catalyst that is formed from the decomposition products of RDX. This conclusion is based on the temporal behaviour of the gas formation rates of the decomposition products. However, from more recent experiments with the independently synthesised mononitroso analogue of RDX, ONDNTA, it appears that this fourth channel may also involve the ONDNTA intermediate. The third and fourth reaction

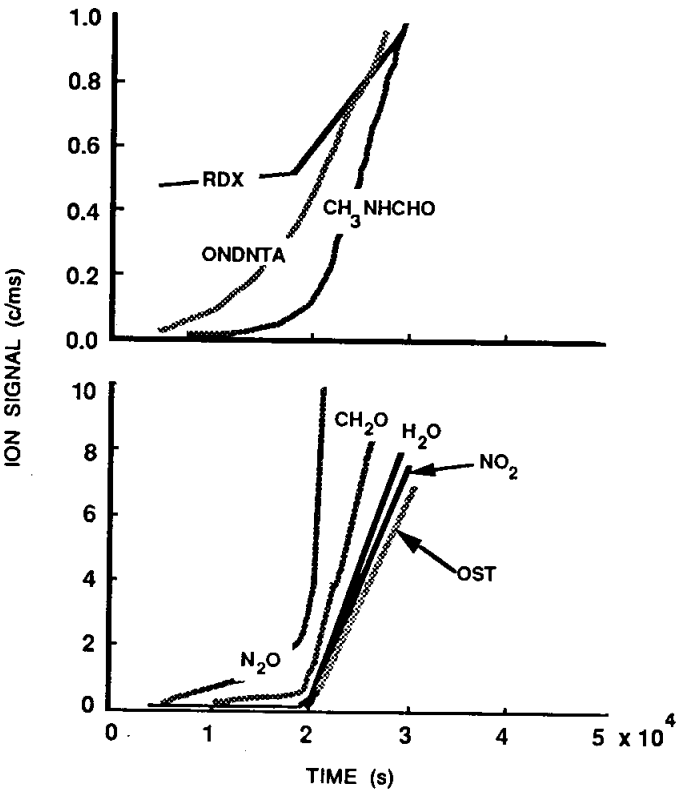

Figure 3. Ion signals associated with the thermal decomposition products formed from pure unlabeled RDX at an isothermal temperature of 190°C. The ONDNTA, N_2O, CH_2O, CH_3NHCHO signals all show a gradual increase prior to the onset of the appearance of the signals associated with the liquid phase decomposition (OST, H_2O and NO_2). Data from Ref. 19.

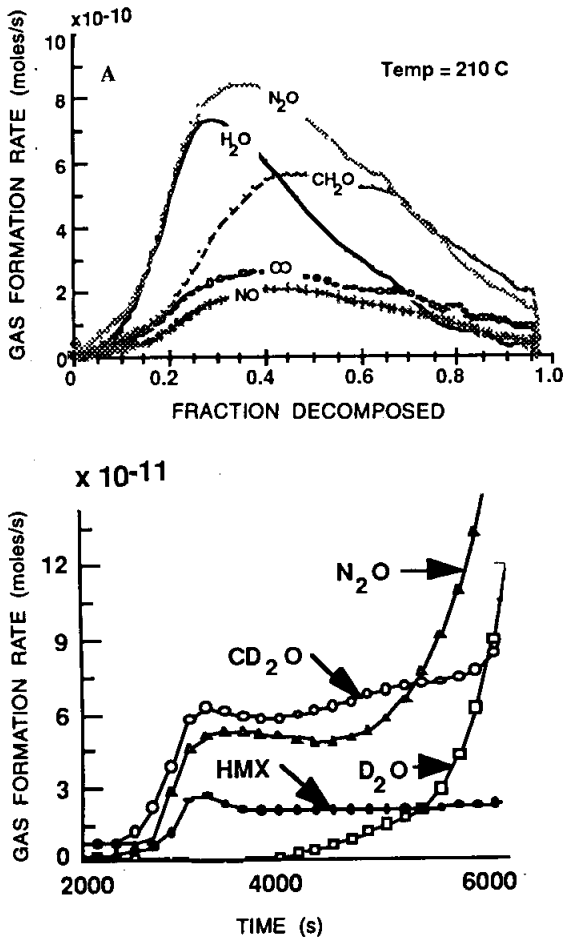

Figure 4. (A) Gas formation rates of the products from the thermal decomposition of HMX at 210 °C. The duration of the decomposition process is about 37000 seconds. (B) Gas formation rates of thermal decomposition products from HMX-d_8 during the induction period and first stage of the acceleration period.

channels each account for approximately 30 per cent of the decomposed RDX.

3.2 RDX Decomposition in the Solid Phase

Experiments with solid phase RDX have shown that its decomposition rate is very much slower than that of liquid phase RDX as can be seen in Fig. 3. ONDNTA is the only product that appears to be formed during the early stages of the decomposition of RDX in the solid phase. As the solid-phase decomposition progresses, N_2O and lesser amounts of CH_2O start to evolve and their rates of evolution increase slowly until products associated with the liquid-phase RDX decomposition appear and the rates of gas formation of all products rapidly increase. This behaviour strongly suggests that the decomposition of solid RDX occurs through formation of ONDNTA within the lattice. Its subsequent decomposition within the lattice to N_2O and CH_2O, followed by the dispersion of CH_2O in the RDX, leads to the eventual liquefaction of the remaining RDX and the onset of the associated liquid-phase decomposition reactions.

3.3 HMX Decomposition in the Solid Phase

The solid phase decomposition of HMX was studied in detail in the temperature range 210 °C and 235 °C. Since its melting point is about 275 °C, the decomposition in the experiments was predominantly in the solid phase. It was found on the basis of temporal correlations of evolution of products that physical processes played a very important role in controlling the rates of decomposition. The first step in the decomposition appeared to be some gas phase decomposition giving rise to products observed as they exit the reaction cell. Concurrently, decomposition occurs in the solid phase, first forming the mononitroso analogue ONTNTA which then decomposes to low molecular weight products. All these products are presumably trapped within the HMX particles initially, forming bubbles containing N_2O and solutions between HMX and CH_2O which could be localised in the volumes surrounding the bubbles. A polymeric product is also formed in the region of the bubbles and itself undergoes a thermal decomposition process yielding low molecular weight products as well as some polymeric residues. Eventually, the size of the bubbles and the pressure within grow, leading to the cracking of the HMX particles and release of the trapped products.

There was also clear experimental evidence that the HMX decomposition was an autocatalytic process as illustrated in the selected plots of gas formation rates shown in Fig. 4. The extent of this autocatalytic effect was shown to be controlled by the reaction of gaseous products with the unreacted HMX, by comparing the rates of formation of products obtained with 5 and 100 mm exit orifices on the reaction cell, respectively. Autocatalysis was much more pronounced when the gaseous products were more confined in the reaction cell.

The thermal decomposition reactions of HMX in the solid phase may also be divided into four groups of

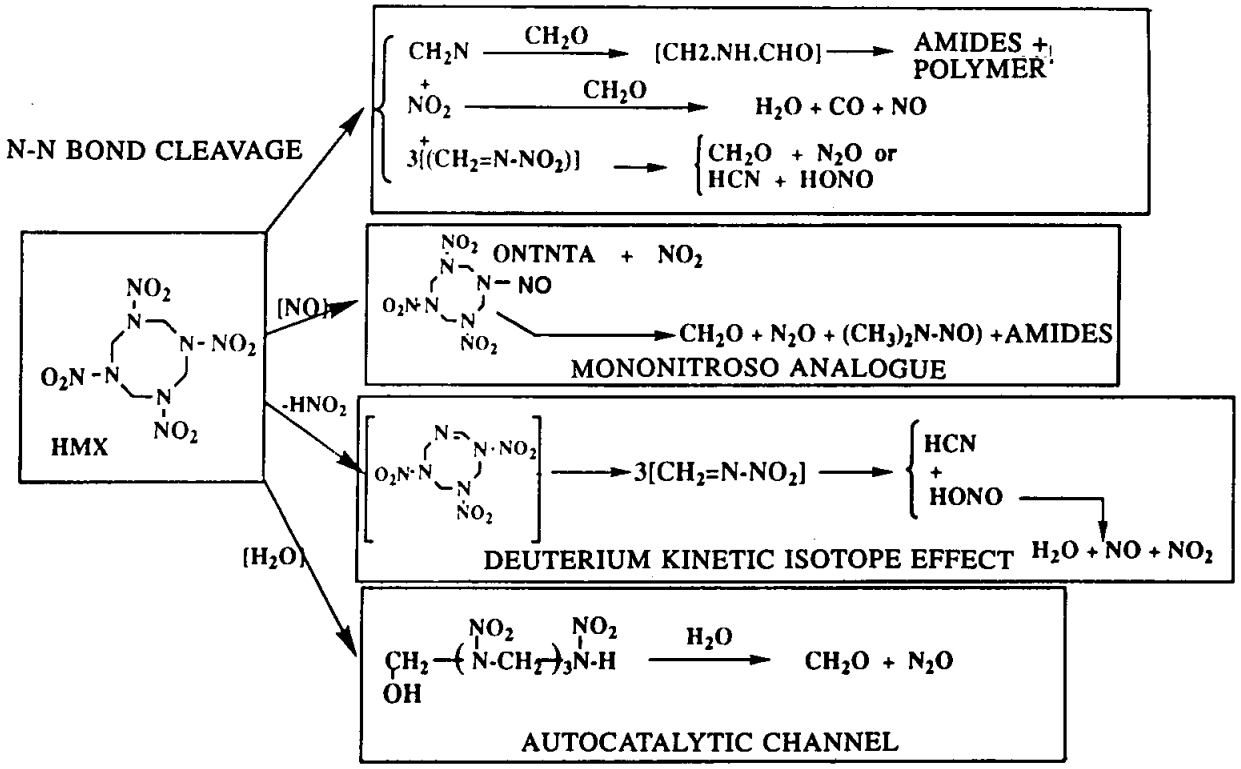

Figure 5. Summary of the proposed reaction pathways controlling the thermal decomposition of HMX in the solid phase. In this scheme, 'methylenenitramine' [CH_2=N-NO_2] is merely assumed intermediate which was actually not detected in the mass spectrometer.

reactions for simplification, constituting four pathways summarised in Fig. 5.

However, some overlap clearly exists between the four branches of the decomposition. One pathway proceeds through *N-N* bond cleavage giving NO_2, CH_2N, and three methylene nitramine intermediates. In a second pathway, an NO_2 group is replaced by an *NO* group forming the mononitroso analogue of HMX. In a third pathway, a hydrogen atom transfers to the adjacent NO_2 group giving rise to the observed deuterium kinetic isotope effect and making it a rate-limiting step. A detailed discussion of these reactions and a description of isotope scrambling and deuterium kinetic isotope effect studies is given in Refs. 17 and 18.

3.4 HMX Decomposition in the Liquid Phase

Comparison of the liquid phase decomposition of HMX with that of RDX will show whether decomposition pathways similar to RDX control the decomposition of HMX or whether the higher melting point of HMX and its decomposition in the solid phase prior to melting alter its decomposition mechanism. The liquid phase decomposition products from HMX observed in our experiments include H_2O, *HCN*, *CO*, CH_2O, *NO*, N_2O, NO_2, formamide, *N*- methylformamide (NMFA), *N,N*-dimethylformamide, and ONTNTA (Fig. 5). In addition, we observe ion signals at m/z values of 70 and 97. Experiments with ^2H, ^{13}C and ^{15}N isotopically labeled HMX analogues have shown that the ion signals at these two m/z values correspond to ions with formulae of $C_2N_2H_2O$ (70) and $C_3N_3H_3O$ (97). For RDX, the ion signals at m/z values of 70 and 97 both arise from the decomposition product, OST. However, for HMX, differences in the relative intensities of these two ions, in addition to differences in their temporal behaviour in the HMX experiments, indicate that they arise from two different decomposition products. These ion signals clearly arise from thermal decomposition products that are similar to the OST formed during the decomposition of RDX. However, without time-of-flight (TOF) velocity-spectra measurements of these ion signals, it is not possible to determine whether the observed ion signals correspond to molecular ions, and thus have the same formula as the thermal decomposition products, or whether they are from daughter ions formed from a decomposition product with a higher molecular weight. In either case, the ion signals at m/z values of 70 and 97 are associated with fragments from the HMX ring formed in a manner similar to reaction pathway P1 for the RDX decomposition (Fig. 2).

The results shown for the decomposition of HMX in Fig. 6 are consistent with the four decomposition

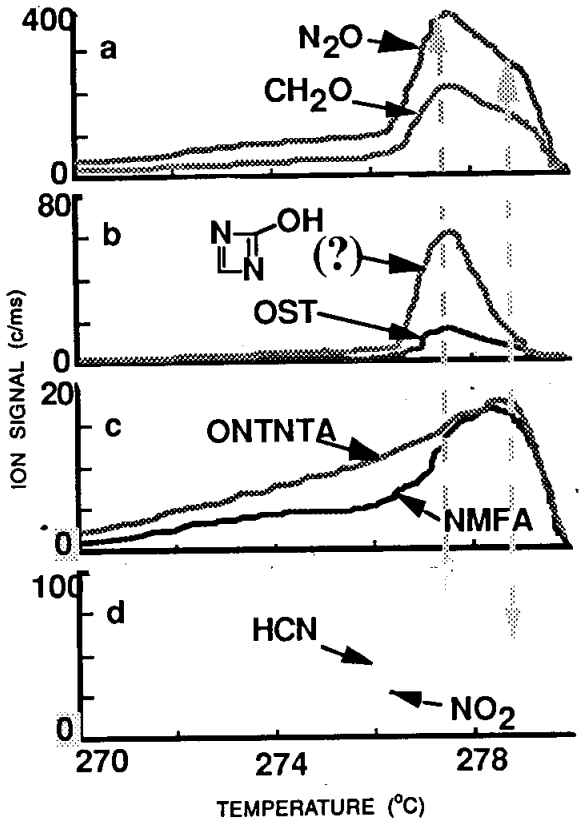

Figure 6. Ion signals associated with various thermal decomposition products formed during the decomposition of HMX as the sample melts. The sample melts at 276 °C. The signals associated with the thermal decomposition fragments of the ring (panel b) only appear in significant quantities as the sample melts. Other products associated with this pathway are indicated by the vertical arrow on the left. After the sample melts, a second set of products that peak later in the decomposition is observed,as indicated by the arrow on the right. These products are associated with the amides, such as the *N*-methylformamide. The heating rate was 2 °C/min.

pathways found for the decomposition of RDX (Fig. 2). A reaction pathway similar to reaction pathway P1 for RDX produces the HMX-ring fragments that are characterised by the ion signals at m/z values of 70 and 97 shown in Panel b of Fig. 6. These two ion signals first appear when the HMX sample liquefies at approximately 276 °C and their signal strengths decrease as the HMX sample is depleted. This behaviour is similar to that observed for OST formed in the decomposition of RDX. The temporal behaviour of the ion signals formed from the mononitroso analogue of HMX, ONTNTA, (shown in Panel c of Fig. 6) is similar to the temporal behaviour

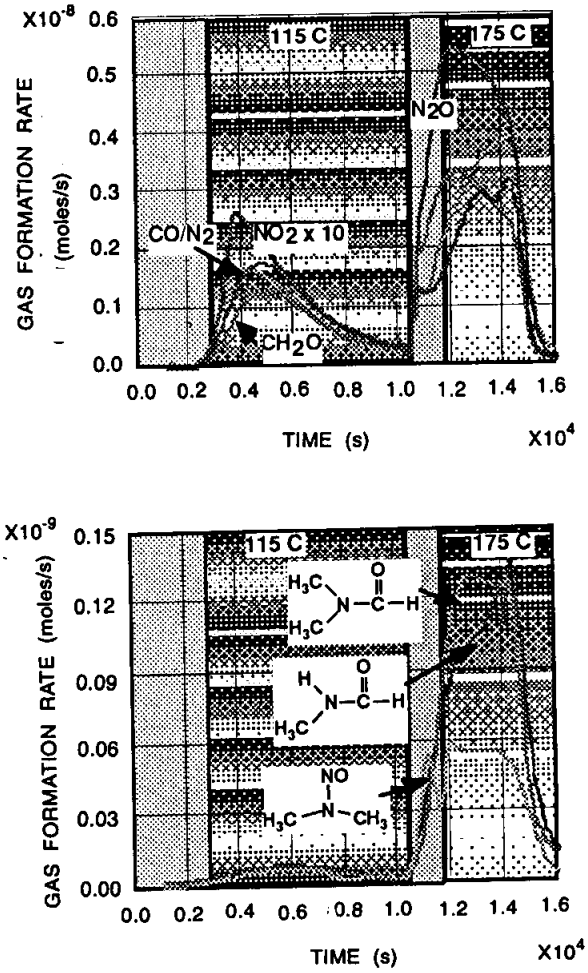

Figure 7. Gas formation rates of decomposition products from the thermal decomposition of ONDNTA in a reaction cell with a 50 μm orifice at isothermal temperatures of 115 °C and 175 °C.

of ONDNTA observed in the liquid-phase RDX decomposition. One significant difference is that a much larger amount of ONTNTA is released from the HMX sample before it liquefies. As can be seen from Fig. 6, the size of the ion signal associated with the ONTNTA product does not show a significant increase as the sample liquefies. This indicates that the decomposition of HMX to its mononitroso analogue is a major decomposition pathway in the solid phase. This is similar to the decomposition of RDX in the solid phase, except that at the higher temperatures associated with the decomposition of HMX, the reaction rate for the formation of ONTNTA is greater and a larger fraction of the HMX sample has decomposed via, a reaction pathway similar to pathway P3 prior to the liquefaction of the HMX sample. The temporal behaviour of the ion

signals associated with the CH_2O and N_2O formed during the decomposition of HMX after its liquefaction, have the same broad type of peaks that were observed for these products in the decomposition of RDX. Both the ion signals associated with these products show a rapid increase as the HMX liquefies. The CH_2O and N_2O formed later in the decomposition appear to be correlated with the ONTNTA product and they also display a temporal behavior that is characteristic of an autocatalytic decomposition channel similar to pathway P4 for RDX.

The initial increase in the CH_2O and N_2O signals after the HMX sample liquefies is also similar to that observed in the decomposition of RDX and associated with decomposition via, reaction pathway P2. From the relative sizes of the ion signals associated with the CH_2O and N_2O products and those associated with the HMX ring fragment ion signals at m/z values of 70 and 97 would suggest that the amount of HMX that decomposes by a pathway similar to P2 compared to pathway P1 is greater for HMX than for RDX. In the light of the fact that the decomposition of HMX occurs at a temperature about 70 °C greater than RDX, the behavior of CH_2O and N_2O tends to suggest that reaction pathway P2 may become more dominant than reaction pathway P1 at higher temperatures. However, it is also possible that the increase of the CH_2O and N_2O signals after the HMX sample liquefies is due to an increase in the decomposition rate of ONTNTA, formed in the solid-phase decomposition. Without further quantification of the HMX results, it is not possible at this time to determine exact relative decomposition rates of the various HMX decomposition products

4. THERMAL DECOMPOSITION OF NITRAMINES (III) to (VIII)

4.1 ONDNTA (III) Decomposition

ONDNTA, the intermediate in RDX decomposition, was independently synthesised[25] to study its decomposition[21] separately. This nitramine uniquely decomposes in two separate temperature regions sequentially, one between 95 and 145 °C and the other between 155 and 210 °C. An illustration of this behaviour is shown in Fig. 7 for the decomposition of ONDNTA in a reaction cell with a 50 mm diameter orifice and held at two different isothermal temperatures. The major decomposition products are N_2O, CH_2O, CO/N_2 and NO_2 and the minor ones include several formamides and dimethylnitrosamine, $(CH_3)_2NNO$. The products obtained from both regions are very similar to those obtained from the decomposition of HMX and RDX in the solid phase with some variation between the two channels of decomposition. It is not understood why the decomposition stops in the intermediate temperature region. However, it is surmised that in this temperature region there is a competition between two processes. One is an autocatalytic process in which gas-phase decomposition products accelerate the decomposition process and the second is some undetectable phase transition that leads to a more stable phase of ONDNTA that is not susceptible to autocatalysis. In support of this conclusion, comparison of the decomposition of ONDNTA in experiments conducted in the reaction cell with 5 mm and 50 mm diameter orifices, respectively, showed that the decomposition occurs 100 times more rapidly with the 5 mm orifice and that the entire sample is consumed in the low temperature channel, presumably due to the autocatalysis by the products.

The behaviour of the decomposition process of ONDNTA under high confinement is illustrated by the data in Fig. 8. The temporal behaviour of the rates of formation of the gaseous products is characterized by two regions. The first region starts at approximately 110 °C and peaks at 125 °C. The second region starts at approximately 140 °C and peaks at 145 °C. A similar temporal behaviour in the two regions was observed during the decomposition of ONDNTA at isothermal temperatures in the 110 to 150 °C range. Thus, it appears that the observed gaseous thermal decomposition products are formed in a series of steps and it is not necessary to increase the temperature as was done in the experiment shown in Fig. 8. The first step in the process leads to the release of CO/N_2 and NO_2 as can be seen from the ion signals in Fig. 8b. These two signals rise and fall sharply. The N_2O and CH_2O signals also rise sharply but decline much more gradually. At 140 °C, after approximately 70 per cent of the sample has decomposed, there is a rapid rise in the rate of formation of a new set of decomposition products as seen in Fig. 8c and 8d. These products include H_2O, *N*-methylformamide, *N,N*-dimethylformamide and dimethylnitrosamine. After the sample stops losing gaseous products, between 5 and 10 per cent of the sample remains as a residue.

These results indicate that as ONDNTA decomposes, it gives gaseous products as well as a

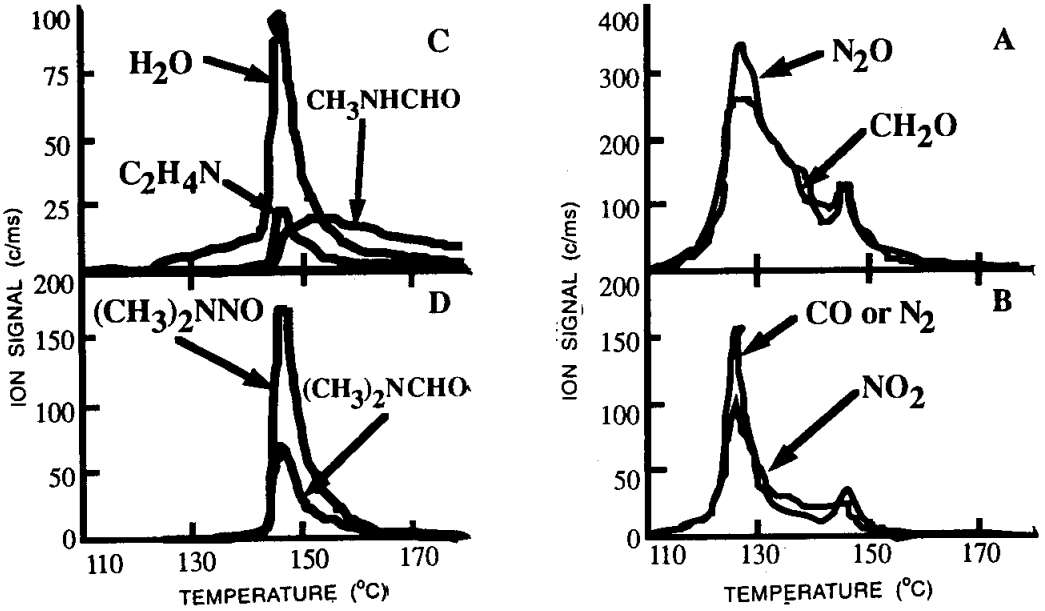

Figure 8. Ion signals in the mass spectrometer from thermal decomposition products of ONDNTA under conditions of high confinement. The heating rate was 2 °C/min.

non-volatile compound (possibly polymeric) that is relatively stable. The first step in the process is likely to be scission of the *N-NO2* bond as evidenced by the *NO2* signal, followed immediately by loss of *CO/N2*, *N2O* and *CH2O* as indicated by the simultaneous rapid rise in these signals. Two different explanations are possible for the sharper decrease in the *CO/N2* and *NO2* signals compared to the N_2O and CH_2 signals. The first one is that the ONDNTA sample is rapidly converted to a nonvolatile product (the rate of conversion is characterized by the *NO2* or *CO/N2* signals) that then undergoes a slower decomposition to form *N2O* and *CH2O*. The second possible explanation is that the nonvolatile decomposition product interacts with the remaining ONDNTA, thus providing another decomposition pathway that leads to the release of *N2O* and *CH2O*. The fact that there is an abrupt appearance of a new set of decomposition products later in the process suggests that the first explanation is more likely. This is because the abrupt appearance of the new products occurs in both the thermal ramp and isothermal experiments. It suggests that the nonvolatile product formed in the initial decomposition of ONDNTA itself decomposes, releasing *N2O* and *CH2O* until it reaches a point at which the nonvolatile product becomes sufficiently unstable that it starts to decompose more rapidly into water, dimethylnitrosamine and the formamides. This process is quite consistent with the observed data. A discussion of details of this process will be presented in a future paper.

The similarities between the products and their sequence of formation in the thermal decomposition of ONDNTA under high confinement conditions and the products observed in the decomposition of HMX in the solid phase are quite striking. Firstly, the major products formed in the decomposition are the same, namely *N2O*, *CH2O* and *CO/N2*. Secondly, the products that originate from the decomposition of the nonvolatile product formed in the decomposition of ONDNTA are the same as those observed in the decomposition of HMX in the solid phase [*H2O*, *(CH3)2NNO*, *CH3NHCHO*, and *(CH3)2NCHO*]. Thirdly, a stable residue remains after the decomposition of both the materials.

4.2 Thermal Decomposition of TNCHP

1,3,5-Trinitro-1,3,5-triaza-cycloheptane (TNCHP) is a cyclic nitramine like RDX with an extra carbon atom in the ring. TNCHP is more stable in the liquid phase

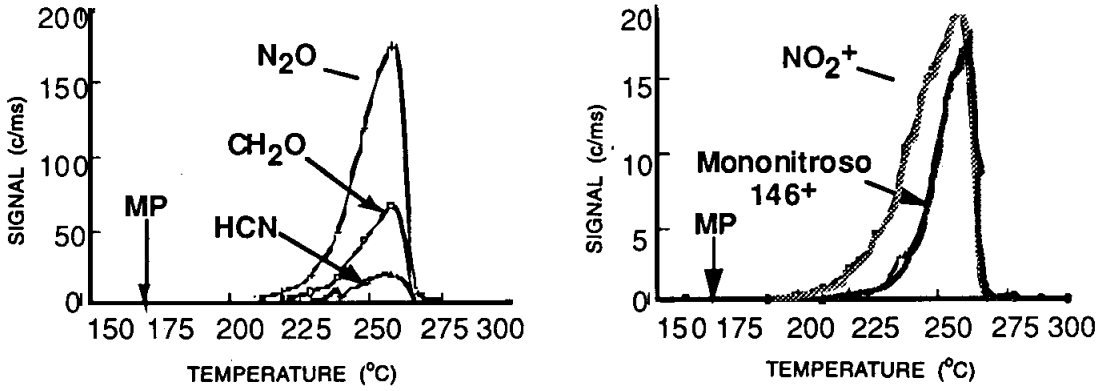

Figure 9. Ion signals associated with the products formed during the thermal decomposition of TNCHP. The heating rate is 2° C/ min.

than either RDX or HMX. The major products formed in its decomposition are CH_2O and N_2O. Products formed to a lesser extent include: H_2O, HCN, NO and NO_2. Ion signals, representing other decomposition products, are also observed. Further measurements utilizing deuterium labeled TNCHP and TOF velocity spectra are underway to determine the identity of the thermal decomposition products leading to these other ion signals. The temporal behaviour of the major ion signals is shown in Fig. 9. These results illustrate the increased thermal stability of TNCHP in the liquid phase as compared to RDX. The ion signal at m/z = 146 is analogous to the ion signal at m/z = 132 that arises from ONDNTA. Thus, the ion signal at m/z =146 most likely belongs to the mononitroso analogue of TNCHP.

In isothermal experiments with TNCHP, the temporal behaviour of the ion signals associated with the decomposition products from TNCHP is indicative of several parallel reaction pathways. The temporal behaviour of several of the products is illustrated in Fig. 10. Ion signals associated with processes that are approximately 'first order' in TNCHP are represented by the signals for NO and NO_2 in Fig. 6 and also include signals that represent HCN. Ion signals associated with intermediate products formed during the thermal decomposition are found at m/z values of 55, 84, 130, and 146. The ion signals at m/z values of 55, 84 and 130 have temporal behaviour similar to that of the signal at m/z = 146, which probably represents the mononitroso analogue of TNCHP. This suggests that the ion signals at m/z values of 55, 84 and 130 may be ion dissociation products of the TNCHP mononitroso analogue. TOF velocity spectra signals at these m/z values will resolve

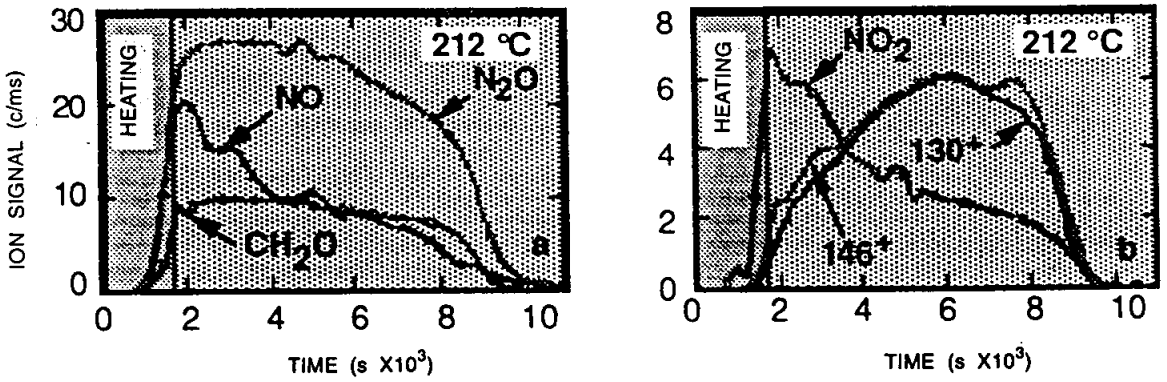

Figure 10. Ion signals associated with the thermal decomposition products from TNCHP. The region in the left shaded panel is the heating portion and the right shaded panel is the isothermal portion of the experiment. The ion signals representing NO and NO_2 appear to be approximately 'first order' in liquid phase TNCHP. The ion signals at m/z values of 130 and 146 are associated with an intermediate formed during the thermal decomposition. The ion signals associated with CH_2O and N_2O probably originate from pathways associated with both the 'first order' process and the decomposition of the intermediate.

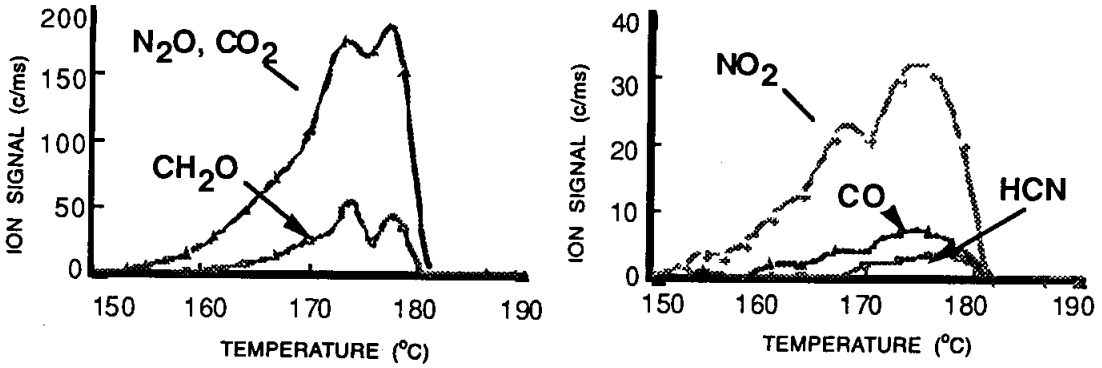

Figure 11. Ion signals formed in the mass spectrometer from products of thermal decomposition of K6.

whether these signals are ion dissociation products formed in the mass spectrometer or whether they arise from additional thermal decomposition products.

A stable product, similar to OST in the decomposition of RDX, was not observed in the thermal decomposition of TNCHP. This inability to form a decomposition product by stabilizing the ring of the cyclic nitramine may be responsible for the increased thermal stability of TNCHP.

4.3 Thermal Decomposition of the Nitramine, K6

The decomposition of K6 is quite different from the other cyclic nitramines used in this study. In addition to its lower thermal stability, K6 also produces fewer and simpler decomposition products. The decomposition products are mainly CH_2O, N_2O and CO_2, with minor contributions from HCN, CO, NO and NO_2.

Unlike the other cyclic nitramines used in this study, K6 does not form any amides, the mononitroso analogue, or a residue. The temporal behaviour of the products formed during the decomposition of K6 is shown in Fig. 11.

The decomposition of K6 (VII) may have been initiated by attack of one of the NO_2 oxygen atoms on the keto group carbon atom, leading to the initial elimination of CO_2 followed by rapid transformation of the remaining fragment into CH_2O and N_2O. The rate of decomposition of K6 through this initial four-centre

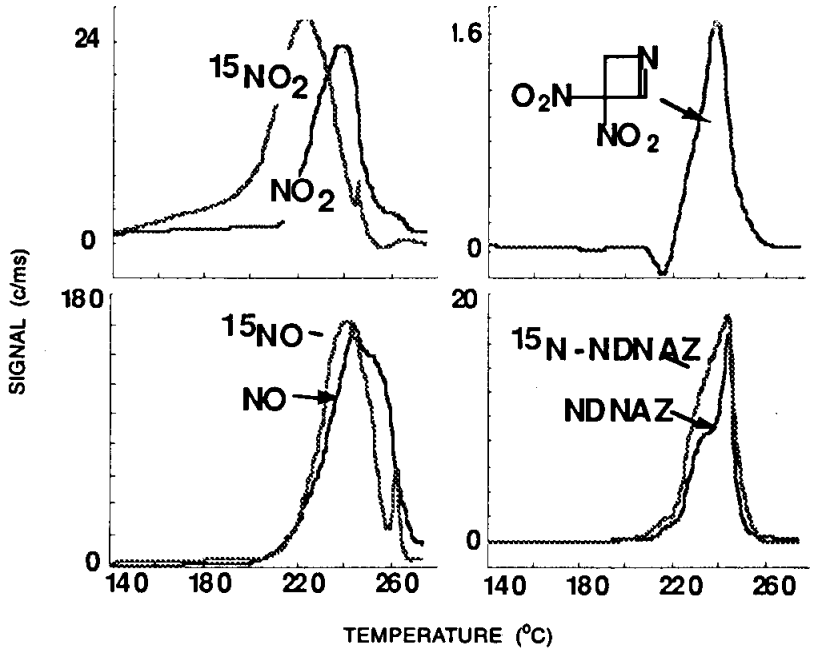

Figure 12. Temporal behaviour of the products formed during the thermal decomposition of TNAZ-1$^{15}NO_2$.

C-N-N-O complex would appear to be competitive with *N-NO2* bond breaking in that no mononitroso analogue or amide products were observed. A more detailed investigation of K6 is currently in progress.

4.4 Thermal Decomposition of the Nitramines, DNCP (V) & DNCHX (VI)

1,3-Dinitro-1,3-diaza-cyclopentane (DNCP) and 1,4-dinitro-1,4-diaza-cyclohexane (DNCHX) are two nitramines with 5- and 6- membered rings, respectively. Only preliminary details of their decompositions are available at present. They exhibit multiple reaction pathways like RDX and HMX, including the formation of the mononitroso analogues[22]. DNCP is thermally much more stable in the molten state as compared to RDX and HMX while DNCHX (VI) begins to decompose in the solid state similar to the case of HMX. DNCP is exceptional in that it does not give rise to the typical nitramine decomposition products, *CH2O* and *N2O*. Further work on the decomposition mechanism of these nitramines is in progress.

4.5 Thermal Decomposition of TNAZ (VIII)

The last nitramine in Fig. 1 that is being investigated[23], is 1,3,3-trinitro-azetidine (TNAZ) (VIII). This is currently under development as a castable explosive because of its low melting point (100 °C) and unusual thermal stability in its molten state. It is an interesting molecule in that it combines a nitramine and a gem-dinitro [*C-(NO2)2*] functional groups. In fact, there is a separate paper[32] which gives further details of its decomposition than what is given here. Briefly, the major products formed are *NO2, NO, H2O, HCN, CO/N2, CO2*, and NDNAZ (1-nitroso-3, 3-dinitroazetidine). Hardly any *N2O* and *CH2O* have been detected unlike in the case of the products of RDX and HMX. This study has shown that, in common with RDX and HMX, the nitroso analogue, NDNAZ, plays an important role as an intermediate in the decomposition of TNAZ. The temporal correlations of the decomposition products from TNAZ-1-$^{15}NO_2$, shown in Fig. 12 suggest a different evolution sequence of product groups and at least four different reaction pathways. As an example, the rate of formation of *NO2* increases first followed by a rise in the rate of formation of *NO* and finally, a rise in the rate of formation of NDNAZ. This observation supports the previous conclusion that the nitroso analogue is formed by an initial cleavage of the *N-NO2* bond followed by the re-attachment of *NO* to the ring, as in the case of RDX and HMX. Decomposition of this sample labeled with $^{15}NO_2$ in the nitramine group, showed that *NO2* originates from both the nitramine and the gem-dinitro groups in the molecule but that the severance of *NO2* from the nitramine group precedes that from the *C-(NO2)2* group. This can be seen clearly in Fig. 12. As a consequence, the ion signals of ^{15}NO and ^{15}N-NDNAZ are also temporally ahead of those from the unlabeled ones which originate from the *C-NO2* groups.

5. CONCLUSION

The comparison of the eight nitramine decompositions studied thus far reveals that the pathway proceeding through the formation of the nitroso analogue is of paramount importance in RDX and HMX and also seems to be significant in the thermal decompositions of four other nitrarnines (IV, V, VI and VIII). It is not yet known whether the cleavage and reformation of *N-NO* bond seen in RDX and HMX is general to all nitramines since this determination preferably requires synthesis of all the nitramines labeled with nitrogen-15. In at least three nitramines studied (V, VI and VIII) the decomposition products commonly observed from nitramines, namely, *CH2O* and *NO2*, are not formed or are formed only in very minute amounts among the products. The implications of these differences and similarities among several nitramines are being explored and investigated further. Thus, this initial comparative study has provided, for the first time, a basis for the study of structure and stability/sensitivity correlations within the class of nitramines, which is the goal of these studies in the search for materials superior to RDX or HMX in overall performance. On the basis of available evidence, it appears that TNCHP is considerably less sensitive than RDX with only a slight trade-off in energy output and it is relatively stable in the molten state. It thus exhibits a potential to be a new useful nitramine with valuable applications.

ACKNOWLEDGEMENTS

The authors wish to thank D.M. Puckett for assistance in collecting the mass spectrometry data and Dr Philip Pagoria for a sample of K6. This work was supported by the Memorandum of Understanding (MoU) between the Office of Munitions and the U.S. Department of Energy under contract DE-AC04-94 AL85000 and between the U.S. Army ARDEC and the U.S. Army Research Office, under contract.

REFERENCES

1. Robertson, A. J. B., *Trans. Faraday Soc.*, 1949, **45**, 85.
2. Rauch, F. C. & Fanelli, A. J. *J. Phys. Chem.*, 1969,73,1604.
3. Cosgrove, J. D. & Owen, A. J. *Combust. Flame*, 1974, **22**, 13 & 19.
4. (a) Batten, J. J. & Murdie, D. C. *Aust. J. Chem.*, 1970, **23**, 737; 749. (b) Batten, J.J. *Aust.J. Chem.*, 1971, **24**, 945 & 2025; 1972, **25**, 2337.
5. Bulusu, S. & Graybush, R.J. Proceedings of the 36th International Congress on Industrial Chemistry, Brussels, Belgium, 1967. *C. R. Ind. Chim.* Belge, 1967, **32**, 647.
6. Bulusu, S.; Graybush, R.J. & Autera, J. R. *Chem. & Ind.(London)*, 1967, 2177.
7. Stals, J. *Trans. Faraday* Soc., 1971, **67**, 1768.
8. Goshgarian, B. B. Airforce Rocket Propulsion Laboratory Report, 1976. AFRPL-TR-78-76.
9. Farber, M. & Srivastava, R. D. *Chem. Phys. Lett.*, 1979, **64**, 307.
10. (a) Axworthy, A. E.; Flanagan, J. E. & Woolery, D. O. Proceedings of the 15th JANNAF Combustion Meeting, CPIA Publication 297. Chemical Propulsion Information Agency, Laurel, MD, 1978, Vol II. p. 253. (b) Axworthy, A. E.; Flanagan, J. E.; Woolery, D. O. & Gray, J. C. Proceedings of the 15th JANNAF Combustion Meeting, CPIA Publication 308, Chemical Propulsion Information Agency, Laurel, MD, 1979, Vol III. p. 289.
11. Oyumi, Y. & Brill, T. B. *Combust. Flame*, 1985, **62**, 213.
12. Hoffsommer, J. C.; Glover, D. J. & Elban, W. L. *J. Energ. Materials*, 1985, **3**, 149.
13. Sharma, J.; Hoffsommer, J. C.; Glover, D. J.; Coffey, C. S.; Forbes, J. W.; Liddiard, T. P.; Elban, W. & Sandiego, F. Proceedings of the Eighth Symposium(International) on Detonation, Albuquerque, NM, 1985. p. 725.
14. (a) Boggs, T.L. The thermal decomposition behavior of cyclotrimethylene-trinitramine(RDX) and cyclotetramethylene- tetranitramine (HMX). In Fundamentals of Solid-Propellant Combustion, Progress in Astronautics and Aeronautics, Vol. 90., edited by K.K. Kuo, and M. Summerfield. AIAA Inc., New York, NY, 1984. (b) Fifer, R. A., p. 177.
15. (a) Schroeder, M.A. Critical Analysis of Nitramine Decomposition Data: Product Distributions from HMX and RDX, BRL- TR-2659, 1985. b) Critical Analysis of Nitramine Decomposition Data: Activation Energies and Frequency Factors for HMX and RDX Decomposition, BRL-TR-2673, 1985.
16. (a) Behrens, R. Jr. *Rev. Sci. Instrum.*, 1986, **58**, 451. (b) Behrens, R. Jr. The application of simultaneous thermogravimetric modulated beam mass spectrometry and time-of-flight velocity spectra measurements to the study of the pyrolysis of energetic materials, in "Chemistry and Physics of Energetic Materials", edited by S.N. Bulusu,; Proceedings of the NATO Advanced Study Institute, Vol. 309. Kluwer Academic Publishers, Netherlands. 1990. p. 327.
17. Behrens, R. Jr. *J. Phys. Chem.*, 1990, **94**, 6706.
18. Behrens, R. Jr. & Bulusu, S. *J. Phys. Chem.*, 1991, **95**, 5838.
19. Behrens, R. Jr. & Bulusu, S. *J. Phys. Chem.*, 1992, **96**, 8877.
20. Behrens, R. Jr. & Bulusu, S. *J. Phys. Chem.*, 1992, **96**, 8891.
21. Behrens, R. Jr.; Land, T. & Bulusu, S. Proceedings of 30th JANNAF Combustion Meeting, Monterey, CA, November 1993.
22. Behrens, R. Jr. & Bulusu, S. Proceedings of 29th JANNAF Combustion Meeting, Hampton, VA, October, 1992.
23. Behrens, R. Jr. & Bulusu, S. Proceedings of 32nd JANNAF Combustion Meeting, Huntsville, AL, October, 1995.
24. Bulusu, S.; Autera, J. R. & Axenrod, T. *J. Labeled Compds. & Radiopharm.*, 1979, 17(5), 707.
25. Brockman, F. J.; Downing, D. C. & Wright, G. F. *Can. J. Res.*, 1949, **27B**, 469.
26. Boyer, J. H. & Kumar, G. J. *Labeled Compds. & Radiopharm.*, 1985, **22**, 1.

27. Meyers, G. S. & Wright, G. F. *Can. J. Res.*, 1949, **27B**, 489.

28. Goodman, L. *J. Am. Chem.* Soc., 1953, **75**, 3019.

29. Chute, W.D.; Herring, K.G.; Toombs, L.E. & Wright, G. F. *Can. J. Res.*, 1948, **26B**, 80.

30. Mitchell, A. R.; Pagoria, P. F.; Coon, C. L.; Jessop, E. S.; Poco, J. F.; Tarver, C. M.; Breithaupt, R.D. & Moody, G.L. Synthesis, Scale-up, and Characterization of K-6. University of California Report,, February, 1991. UCRL-LR-109404.

31. Archibald, T.G.; Gilardi, R.; Baum, K. & Cohen, M.C. *J . Org. Chem.*, 1990, **55**, 2920.

32. Behrens, R. Jr. & Bulusu, S. Proceedings of the International Seminar on High Energy Materials, 19-21 November, 1996, Pune, India.